

Received 10 July 2021; revised 17 August 2021; accepted 26 August 2021. Date of publication 30 August 2021; date of current version 13 December 2021.
The review of this paper was arranged by Editor B.-Y. Nguyen.

Digital Object Identifier 10.1109/JEDS.2021.3108854

Subthreshold Swing in Silicon Gate-All-Around Nanowire and Fully Depleted SOI MOSFETs at Cryogenic Temperature

SHOHEI SEKIGUCHI, MIN-JU AHN^{1b}, TOMOKO MIZUTANI^{1b}, TAKUYA SARAYA (Member, IEEE),
MASAHARU KOBAYASHI^{1b} (Member, IEEE), AND TOSHIRO HIRAMOTO^{1b} (Member, IEEE)

Institute of Industrial Science, The University of Tokyo, Tokyo 153-8505, Japan

CORRESPONDING AUTHOR: T. HIRAMOTO (e-mail: hiramoto@nano.iis.u-tokyo.ac.jp)

This work was supported by the Japan Society for the Promotion of Science (JSPS) KAKENHI under Grant JP19H00754.

ABSTRACT Subthreshold swing (SS) in a silicon gate-all-around (GAA) nanowire MOSFET with zero body factor is examined from room temperature (RT) down to 4 K. A fully depleted (FD) SOI MOSFET is also evaluated. The values of SS of both transistors decrease in proportional to temperature (T) but start to saturate below 18K, similar to transistors with non-zero body factor in the literature, indicating that the body factor is not related to the SS saturation phenomena at very low temperatures.

INDEX TERMS Nanowire, MOSFET, subthreshold swing.

I. INTRODUCTION

The quantum computer has attracted much attention for solving certain complex problems much faster than classical computers. In the real applications of quantum computers, qubits will be integrated with large-scale CMOS circuits operating at cryogenic temperatures. Therefore, the characterizations of MOSFETs at cryogenic temperatures become increasingly important. One of the merits of cryogenic temperature MOSFET operation is the suppressed subthreshold leakage current, because subthreshold swing (SS) is given by

$$SS = (k_B T/q) \ln 10 (1 + \gamma), \quad (1)$$

$$\gamma = C_D / C_{ox}, \quad (2)$$

under the assumption that the short channel effect is negligible, where k_B is the Boltzmann constant, T the temperature, q the elementary charge, γ the body factor, C_D the depletion capacitance, and C_{ox} the gate capacitance [1]–[2]. According to Eq. (1), the ideal value of 60 mV/dec at $T = 300\text{K}$ (room temperature) is achieved when $\gamma = 0$. SS decreases in proportion to the temperature and its value should be as small as 0.79 mV/dec at 4K when $\gamma = 0$. However, it has been reported that the measured SS value is not in proportion to the temperature at very low temperatures and

saturates around 10mV/dec [3]–[9]. The reasons for this saturation phenomena have been argued and one of the possible mechanisms would be the increased interface traps at low temperatures [4]–[6], [8]–[9].

In this work, we focused on the effect of body factor (γ) in Eq. (1) on the SS saturation phenomena. γ is given by Eq. (2) and is an indicator of how strongly the body is coupled to the channel. From the electric characteristics point of view, on the other hand, γ is an indicator of the body effect and defined as,

$$\gamma = |V_{TH}/V_{BS}|, \quad (3)$$

where V_{TH} is the threshold voltage and V_{BS} the body voltage [1]–[2]. γ shows how much V_{TH} is shifted by V_{BS} . At given temperature, the minimum and ideal SS is achieved in a transistor with $\gamma = 0$, where the coupling between the gate and the channel is strongly enough and the body coupling is negligible. A gate-all-around (GAA) nanowire transistor, in which the nanowire channel is completely surrounded by the gate electrode, is one of the structures that can attain $\gamma = 0$.

Most of the previous work on the SS measurements at low temperature have been done for transistors with large γ , and few measurements have been reported on transistors with zero body factor. In order to investigate the effect

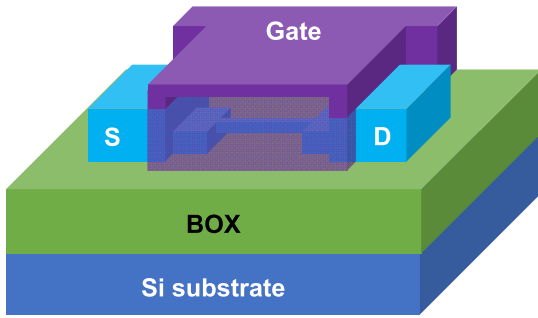


FIGURE 1. A three-dimensional schematic view of a fabricated silicon GAA nanowire MOSFET.

of γ on the SS saturation, we fabricated silicon gate-all-around (GAA) nanowire transistors with $\gamma = 0$ and $SS = 60\text{mV/dec}$ at room temperature and carefully measured SS at various temperatures. As a reference, fully depleted (FD) SOI MOSFETs are also fabricated and evaluated. This paper is the extended version of Reference [10], but all the data in this paper were re-measured and the device temperature was accurately calibrated by a pn diode temperature sensor.

II. DEVICE FABRICATION AND BODY FACTOR

Fig. 1 shows a three-dimensional schematic of the n-type GAA nanowire transistor. The fabrication process is based on references [11]–[12]. An SOI substrate with the SOI thickness of $t_{\text{SOI}} = 80\text{ nm}$ and the buried oxide thickness of $t_{\text{BOX}} = 200\text{ nm}$ was used. The active region of SOI was locally thinned down to 15 nm by oxidation by which source/drain regions remained thick to reduce parasitic resistance. The nanowire pattern was defined by the electron beam lithography and reactive ion etching, followed by the wet-etching process which etches BOX under the nanowire forming a suspending nanowire from BOX. A gate oxide was thermally grown ($t_{\text{ox}} = 7\text{ nm}$) and poly-Si was deposited for a gate electrode by which the GAA structure is formed. Length (L) and width (W) of nanowire are 250 nm and 10 nm , respectively. Effective width (W_{eff}) is the peripheral of the nanowire and is 50 nm . The gate length is $30\mu\text{m}$, so the source/drain edges locate outside of nanowire. The source/drain doping concentration is approximately $2 \times 10^{20}\text{ cm}^{-3}$. For a reference, a planar n-type FDSOI MOSFET with $W = 20\mu\text{m}$ and $L = 30\mu\text{m}$ was also fabricated and evaluated, where $t_{\text{SOI}} = 15\text{ nm}$ in the SOI channel and $t_{\text{SOI}} = 80\text{ nm}$ in source/drain regions.

$I_{\text{DS}} - V_{\text{GS}}$ characteristics were carefully measured with gate voltage (V_{GS}) at an interval of 2.5 mV . Fig. 2 shows measured $I_{\text{DS}} - V_{\text{GS}}$ characteristics with different V_{BS} at room temperature. The $I_{\text{DS}} - V_{\text{GS}}$ curve is shifted by V_{BS} in the FD SOI MOSFET. The γ value is 0.036 , where γ is defined in Eq. (3). On the other hand, the curve is never shifted in the GAA nanowire MOSFET. The zero body factor in the GAA nanowire MOSFET is confirmed.

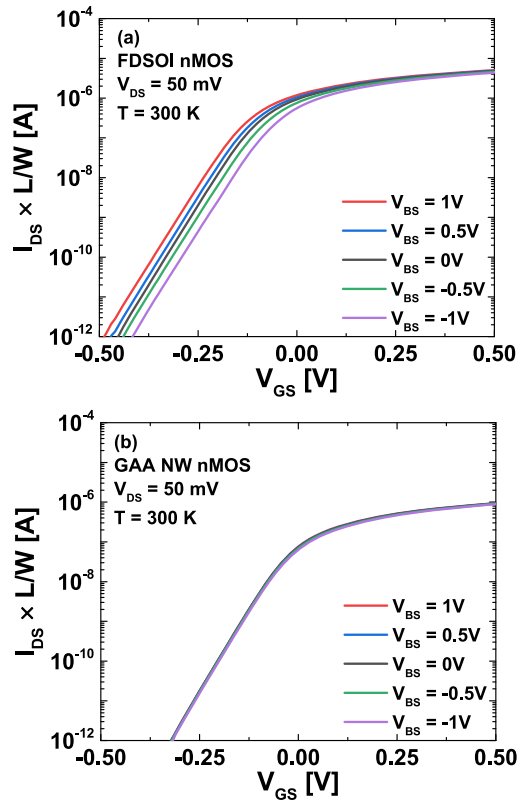


FIGURE 2. Measured $I_{\text{DS}} - V_{\text{GS}}$ characteristics with different V_{BS} at room temperature in (a) FDSOI and (b) GAA nanowire nMOSFETs. V_{DS} is 50 mV . I_{DS} is normalized to W/L for fair comparison, where W_{eff} is used for W in the nanowire MOSFET.

In this study, SS is defined as an average value in the range from $I_{\text{DS}} \times L/W = 10^{-11}$ to 10^{-10} [A] . SS at room temperature is 62.5 mV/dec for the FDSOI MOSFET and 60.45 mV/dec for the nanowire MOSFET. It is confirmed that the GAA nanowire transistor shows an almost ideal value of SS as well as zero body factor at room temperature.

III. CHARACTERISTICS AT CRYOGENIC TEMPERATURE

Fig. 3 shows the temperature dependence of $I_{\text{DS}} - V_{\text{GS}}$ characteristics of the FDSOI and GAA nanowire MOSFETs. As the temperature decreases, V_{TH} increases, drain current at on-state increases, and the subthreshold slope becomes steeper in both FDSOI and GAA nanowire MOSFETs.

Fig. 4 shows the SS values as a function of normalized I_{DS} ($I_{\text{DS}} \times L/W$) in FDSOI and GAA nanowire MOSFETs. SS decreases with the temperature but the decrease in SS becomes gradual below 18 K in both MOSFETs. SS values at 18 K , 10 K , and 4 K are the almost the same in the FDSOI MOSFET. In the nanowire MOSFETs, the oscillations of SS are observed at 10 K and 4 K , and the SS value in the range of $I_{\text{DS}} \times L/W$ from 10^{-11} to 10^{-10} [A] increases at 4 K due to the SS peak. It is found that these oscillations are observed in other nanowire MOSFETs. The oscillations are different depending on nanowire transistors, but in the same nanowire

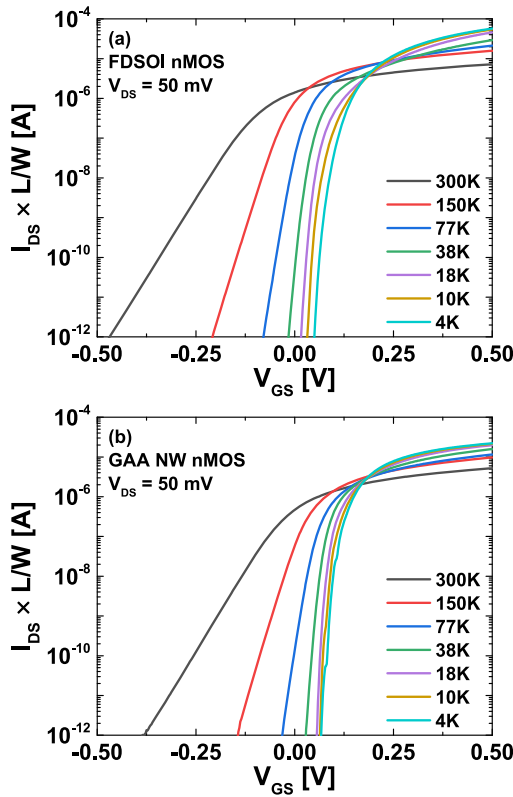


FIGURE 3. Measured subthreshold characteristics at different temperatures from 300K down to 4K in (a) FDSOI and (b) GAA nanowire MOSFETs.

transistor the oscillations are reproducible when repeatedly measured as shown in Fig. 5. The SS oscillations may be caused by the Coulomb blockade due to the potential fluctuation in nanowire channel caused by the slight nanowire width fluctuations [11]. The SS oscillations are never observed in FDSOI MOSFETs.

Fig. 6 shows the SS values as a function of the temperature. The ideal SS with $\gamma = 0$ ($(k_B T/q) \ln 10$) is shown as a straight line. For the FDSOI MOSFETs, SS is slightly larger than the ideal SS line at room temperature. SS decreases along with the ideal SS, starts to deviate at 18K, and almost saturate below 10K. At 18K, SS is 7.5 mV/dec in the FDSOI MOSFETs, which is 2.1 times larger than the ideal value. For the nanowire MOSFETs, SS is on the ideal SS line and decreases along with the ideal SS. At 18K, SS is 4.7 mV/dec in the nanowire MOSFETs, which is 1.3 times larger than the ideal value, indicating that the SS saturation starts at 18K.

The effect of the Coulomb blockade is superimposed below 10K in the nanowire MOSFET, but the SS value smaller than 4.7 mV/dec is not observed in any $I_{DS} \times L/W$ range as shown in Fig. 4(b). It is concluded that the SS saturation at low temperature occurs even in a nanowire MOSFET with $\gamma = 0$. Fig. 6 also shows reported SS in the literature [3]–[8]. Irrespective of SS at room temperature, all transistors show the SS saturation below around 50K.

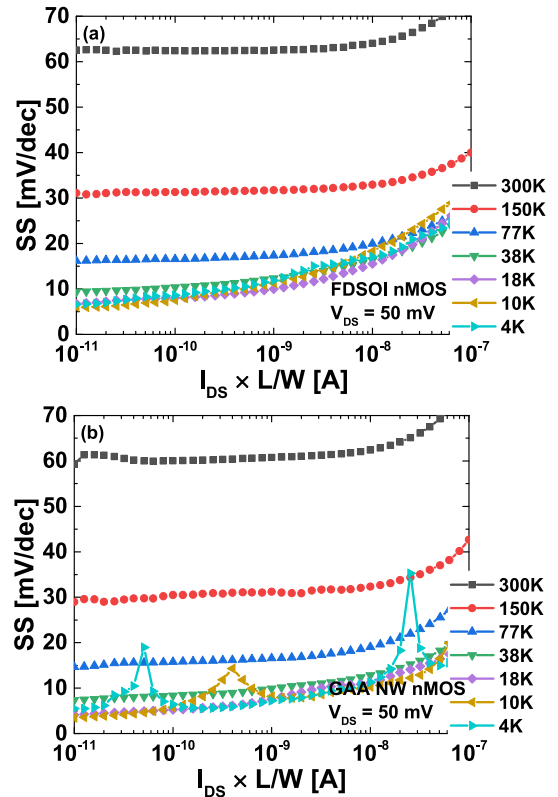


FIGURE 4. Measured SS as a function of normalized I_{DS} at different temperatures in (a) FDSOI and (b) GAA nanowire MOSFETs. SS is defined as an average value between $I_{DS} \times L/W = 10^{-11}$ and 10^{-10} [A].

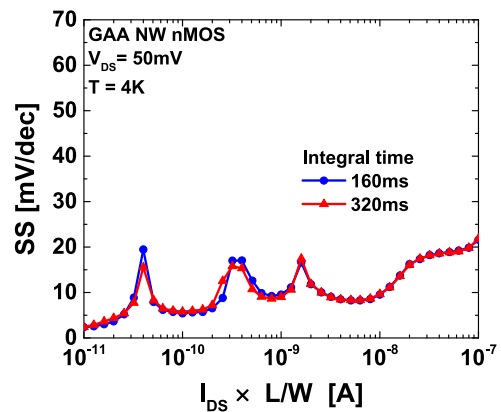


FIGURE 5. Measured SS as a function of normalized I_{DS} at 4K in another GAA nanowire MOSFET. Different oscillations from those in Fig. 4(b) are observed. The oscillations are reproducible even when the measurement integral time is varied.

It is considered that the simple interface trap model cannot explain the observed phenomena either, because one has to assume impossibly high N_{it} ($\sim 10^{16} \text{ cm}^{-2}$) in this model [5]. Recently, the band-tail extension model has been proposed to explain the temperature-independent SS at low temperature [3]. For quantum computing with peripheral large-scale CMOS circuits, accurate device models at low temperature are strongly required.

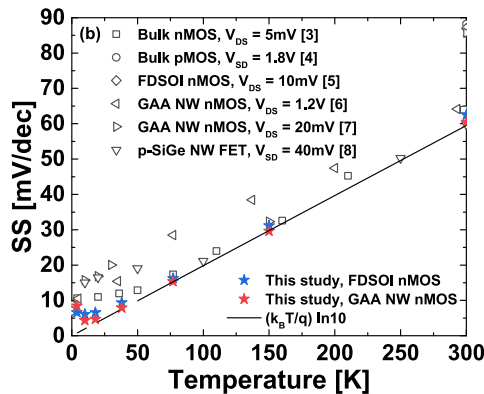


FIGURE 6. Measured SS as a function of the temperatures in FDSOI and GAA nanowire MOSFETs. Reported SS in the literature [3]–[8] are also shown.

IV. CONCLUSION

Subthreshold swing in a GAA nanowire transistor with zero body factor and ideal SS at room temperature was investigated at cryogenic temperature. It is experimentally confirmed that the SS saturation phenomena at low temperatures occurs even in the transistor with no body factor.

REFERENCES

- [1] T. Koura, M. Takamiya, and T. Hiramoto, "Optimum conditions of body effect factor and substrate bias in variable threshold voltage MOSFETs," *Jpn. J. Appl. Phys.*, vol. 39, no. 4B, pp. 2312–2317, Apr. 2000, doi: [10.1143/JJAP.39.2312](https://doi.org/10.1143/JJAP.39.2312).
- [2] T. Ohtou, T. Saraya, and T. Hiramoto, "Variable-body-factor SOI MOSFET with ultrathin buried oxide for adaptive threshold voltage and leakage control," *IEEE Trans. Electron Devices*, vol. 54, no. 1, pp. 40–46, Jan. 2008, doi: [10.1109/TED.2007.912612](https://doi.org/10.1109/TED.2007.912612).
- [3] A. Beckers, F. Jazaeri, and C. Enz, "Theoretical limit of low temperature subthreshold swing in field-effect transistors," *IEEE Electron Device Lett.*, vol. 41, pp. 276–279, Feb. 2020, doi: [10.1109/LED.2019.2963379](https://doi.org/10.1109/LED.2019.2963379).
- [4] R. M. Incandela, L. Song, H. Homulle, E. Charbon, A. Vladimirescu, and F. Sebastiano, "Characterization and compact modeling of nanometer CMOS transistors at deep-cryogenic temperatures," *IEEE J. Electron Devices Soc.*, vol. 6, pp. 996–1006, 2018, doi: [10.1109/JEDS.2018.2821763](https://doi.org/10.1109/JEDS.2018.2821763).
- [5] P. Galy, C. Lemyre, P. Lemieux, F. Arnaud, D. Drouin, and M. Pioro-Ladrière, "Cryogenic temperature characterization of a 28-nm FD-SOI dedicated structure for advanced CMOS and quantum technologies co-integration," *IEEE J. Electron Devices Soc.*, vol. 6, pp. 594–600, 2018, doi: [10.1109/JEDS.2018.2828465](https://doi.org/10.1109/JEDS.2018.2828465).
- [6] N. Singh *et al.*, "Ultra-narrow silicon nanowire gate-all-around CMOS devices: Impact of diameter, channel-orientation and low temperature on device performance," in *Proc. Int. Electron Devices Meeting*, Dec. 2006, pp. 1–4, doi: [10.1109/IEDM.2006.346840](https://doi.org/10.1109/IEDM.2006.346840).
- [7] D. Boudier, B. Cretu, E. Simoen, A. Veloso, and N. Collaert, "On quantum effects and low frequency noise spectroscopy in Si gate-all-around nanowire MOSFETs at cryogenic temperatures," in *Proc. EUROSOCI-ULIS*, Apr. 2017, pp. 5–8, doi: [10.1109/ULIS.2017.7962578](https://doi.org/10.1109/ULIS.2017.7962578).
- [8] B. C. Paz *et al.*, "Cryogenic operation of Ω -gate p-type SiGe-on-insulator nanowire MOSFETs," in *Proc. EUROSOCI-ULIS*, Granada, Spain, Mar. 2018, pp. 1–4, doi: [10.1109/ULIS.2018.8354736](https://doi.org/10.1109/ULIS.2018.8354736).
- [9] H. Oka *et al.*, "Toward long-coherence-time Si spin Qubit: The origin of low-frequency noise in cryo-CMOS," in *Proc. Symp. VLSI Technol.*, Honolulu, HI, USA, Jun. 2020, pp. 1–2, doi: [10.1109/VLSITechnology18217.2020.9265013](https://doi.org/10.1109/VLSITechnology18217.2020.9265013).
- [10] S. Sekiguchi, M.-J. Ahn, T. Saraya, M. Kobayashi, and T. Hiramoto, "Subthreshold swing in silicon gate-all-around nanowire MOSFET at cryogenic temperature," in *Proc. Electron Devices Technol. Manuf. Conf.*, Chengdu, China, Apr. 2021, pp. 1–3, doi: [10.1109/EDTM50988.2021.9420934](https://doi.org/10.1109/EDTM50988.2021.9420934).
- [11] R. Suzuki, M. Nozue, T. Saraya, and T. Hiramoto, "Experimental observation of quantum confinement effect in (110) and (100) silicon nanowire field-effect transistors and single-electron/hole transistors operating at room temperature," *Jpn. J. Appl. Phys.*, vol. 52, Oct. 2013, Art. no. 104001, doi: [10.7567/JJAP.52.104001](https://doi.org/10.7567/JJAP.52.104001).
- [12] M.-J. Ahn, T. Saraya, M. Kobayashi, N. Sawamoto, A. Ogura, and T. Hiramoto, "Superior subthreshold characteristics of gate-all-around p-type junctionless poly-Si nanowire transistor with ideal subthreshold slope," *Jpn. J. Appl. Phys.*, vol. 59, no. 7, Jul. 2020, Art. no. 070908, doi: [10.35848/1347-4065/ab9e7d](https://doi.org/10.35848/1347-4065/ab9e7d).